quantum beam science

MDPI

Article

Time-Resolved Radioluminescence Dosimetry Applications and the Influence of Ge Dopants In Silica Optical Fiber Scintillators

Zubair H. Tarif [1,2], Adebiyi Oresegun [1], Auwal Abubakar [3,4], Azmi Basaif [1], Hafiz M. Zin [3], Kan Yeep Choo [1], Siti A. Ibrahim [1], Hairul Azhar Abdul-Rashid [1,*] and David A. Bradley [5,6]

1 Fiber Optics Research Centre, Faculty of Engineering, Multimedia University, Cyberjaya 63100, Jalan Multimedia, Malaysia; zubair.tarif@gmail.com (Z.H.T.); adeoresegun@hotmail.com (A.O.); az87mi@gmail.com (A.B.); kychoo@mmu.edu.my (K.Y.C.); azlida@mmu.edu.my (S.A.I.)
2 Lumisyns Sdn Bhd, Cyberjaya 63100, Selangor, Malaysia
3 Advanced Medical and Dental Institute, Universiti Sains Malaysia (USM), Kepala Batas 13200, Penang, Malaysia; a.abubakar@unimaid.edu.ng (A.A.); hafiz.zin@usm.my (H.M.Z.)
4 Department of Medical Radiography, University of Maiduguri, Maiduguri 1069, Nigeria
5 Centre for Applied Physics and Radiation Technologies, Sunway University, Bandar Sunway, Petaling Jaya 47500, Selangor, Malaysia; d.a.bradley@surrey.ac.uk
6 Department of Physics, University of Surrey, Guildford GU2 7XH, UK
* Correspondence: hairul@mmu.edu.my

Abstract: The quality of treatment delivery as prescribed in radiotherapy is exceptionally important. One element that helps provide quality assurance is the ability to carry out time-resolved radiotherapy dose measurements. Reports on doped silica optical fibers scintillators using radioluminescence (RL) based radiotherapy dosimetry have indicated merits, especially regarding robustness, versatility, wide dynamic range, and high spatial resolution. Topping the list is the ability to provide time-resolved measurements, alluding to pulse-by-pulse dosimetry. For effective time-resolved dose measurements, high temporal resolution is enabled by high-speed electronics and scintillator material offering sufficiently fast rise and decay time. In the present work, we examine the influence of Ge doping on the RL response of Ge-doped silica optical fiber scintillators. We particularly look at the size of the Ge-doped core relative to the fiber diameter, and its associated effects as it is adjusted from single-mode fiber geometry to a large core-to-cladding ratio structure. The primary objective is to produce a structure that facilitates short decay times with a sufficiently large yield for time-resolved dosimetry. RL characterization was carried out using a high-energy clinical X-ray beam (6 MV), delivered by an Elekta Synergy linear accelerator located at the Advanced Medical and Dental Institute, Universiti Sains Malaysia (USM). The Ge-doped silica optical fiber scintillator samples, fabricated using chemical vapor deposition methods, comprised of large core and small core optical fiber scintillators with high and low core-to-cladding ratios, respectively. Accordingly, these samples having different Ge-dopant contents offer distinct numbers of defects in the amorphous silica network. Responses were recorded for six dose-rates (between 35 MU/min and 590 MU/min), using a photomultiplier tube setup with the photon-counting circuit capable of gating time as small as 1 µs. The samples showed linear RL response, with differing memory and afterglow effects depending on its geometry. Samples with a large core-to-cladding ratio showed a relatively short decay time (<1 ms). The results suggest a contribution of Ge-doping in affecting the triplet states of the SiO_2 matrix, thereby reducing phosphorescence effects. This is a desirable feature of scintillating glass materials that enables avoiding the pulse pile-up effect, especially in high dose-rate applications. These results demonstrate the potential of Ge-doped optical-fiber scintillators, with a large core-to-cladding ratio for use in time-resolved radiation dosimetry.

Keywords: optical fiber scintillators; Ge-doped optical fiber; time-resolved radiation dosimetry; FLASH radiotherapy

Citation: Tarif, Z.H.; Oresegun, A.; Abubakar, A.; Basaif, A.; Zin, H.M.; Choo, K.Y.; Ibrahim, S.A.; Abdul-Rashid, H.A.; Bradley, D.A. Time-Resolved Radioluminescence Dosimetry Applications and the Influence of Ge Dopants In Silica Optical Fiber Scintillators. *Quantum Beam Sci.* **2022**, *6*, 15. https://doi.org/10.3390/qubs6020015

Academic Editors: Klaus-Dieter Liss and William L. Dun

Received: 20 October 2021
Accepted: 21 March 2022
Published: 7 April 2022

1. Introduction

Dosimetry is crucial in ensuring effective radiotherapy and radiation safety within the surrounding environments, forming a key aspect of radiotherapy quality assurance. Currently, real-time radiation dosimetry systems have largely been limited to measuring the dose over the entire beam-on time with little insight into detailed pulse-by-pulse delivery of the prescribed dose [1]. Medical electron linear accelerators (linac) deliver electron and X-ray radiation pulses at a typical repetition frequency of some 30 Hz, potentially reaching up to some 400 Hz in adaptations, and a pulse width of 3–5 μs. The high repetition rate and short pulse width challenge the ability of existing detectors, especially with regards to the recombination and recovery of charges. The ability to measure these individual pulses provides for accurate measurement of beam quality, leading to the measurement of the delivered dose in real-time [2,3].

Recent radiotherapy modalities, such as the ultra-high dose rate FLASH radiotherapy, promise reduction of the total time of dose delivery by delivering, to date having been demonstrated to less than 200 ms, with reduced damage to healthy tissues while delivering therapeutic efficacy to the tumor tissues. Despite such evidence, several FLASH parameters and suitable dosimetry techniques have yet to be established. FLASH dose rates greater than 40 Gy/s will require dose-per-pulse in excess of 1 Gy. This is therefore at least two orders of magnitude greater than the dose-per-pulse produced by conventionally provisioned linacs (dose-per-pulse being in the mGy range in conventional radiotherapy). With a high pulse repetition frequency, the dosimetry system desired for FLASH should be expected to provide for time-resolved measurements, needing to offer a decay time sufficiently short for pulse-by-pulse signal collection, coupled with low saturation properties [4].

Optical fiber scintillators used in radiation dosimetry systems and operating based on radioluminescence (RL) provide for remote, real-time, and in-vivo dosimetry [5,6]. Moreover, the optical fiber-based dosimetry systems are small in cross-section (leading to high spatial resolution) and are immune to electromagnetic interference. The optical fiber scintillator luminesces when exposed to ionizing radiation, albeit with the radiation driven fluorescence component accompanied by a brief period of afterglow following termination of irradiation. The latter can place practical limits on temporal resolution, as will be discussed later. The photons produced are guided through an optical fiber waveguide to a photodetector and photon counting system [7,8]. Several reports on optical fiber-based RL dosimetry systems have been made, based on plastic optical fibers or silica glass optical fibers coupled with different scintillating materials used in both external beam radiotherapy (EBRT) and brachytherapy [9–12]. In related developments, emerging modalities such as synchrotron microbeam radiation therapy (MRT) require dosimetry systems with a high spatial resolution to resolve dose profiles of microbeams comprising collimated X-ray planes with few tens of μm thickness and few hundreds of μm separation between planes [13,14].

Fast decay is critical in efforts towards realizing an optimum pulse sensitive dosimetry system [15,16], the period of decay (defined here as the depletion time of the luminescent signal to noise level) needing to be somewhat shorter than the period between adjacent linac pulses, as illustrated in Figure 1. A typical linac pulse has a duration of 2-8 μs (t_{pulse}), which are delivered with a repetition rate of some tens of Hz, making the temporal difference between two adjacent pulses in the ms range ($t_{interval}$). The three main components of radioluminescence are prompt, fast and slow emission. In addition to the rise time of the emission, t_{rise}, the four timing components that characterize the RL response of a scintillator are thus, t_{rise}, t_{prompt}, t_{fast} and t_{slow}. Generally, the summation of these is desired to be less than the $t_{interval.}$ We have earlier reported on the RL response of Ge-doped silica optical fiber scintillators, a particular candidate for time-resolved dosimetry [17,18]; the composite decay time of the system for both samples, 6 and 10 mol% Ge concentration, was calculated at 50 ms and 40 ms, respectively. While the calculated composite decay time indicates the Ge-doped optical fiber scintillators to have good potential for time-resolved radiation dosimetry (primarily in low dose rates), much more detailed investigation is still required

to further optimize the dosimetry performance in terms of decay time and RL yield. The light yield from Ge-doped silica optical fiber scintillators was found to be sufficiently large in these earlier investigations for dosimetry applications, while the desired decay time needed to be furthered shortened. The desired decay time for scintillators to be used in time-resolved dosimetry need to be sufficiently longer than the nascent fluorescence ($t_{fast} + t_{slow} > t_{prompt}$) from the carrier optical fiber (usually PMMA or silica multimode fibers that contributes to the stem effect) to enable gated measurements, while short enough ($t_{fast} + t_{slow} < t_{interval}$) to accommodate faster pulse repetition rates, suggesting a value for $t_{fast} + t_{slow}$ between 0.1–2 ms [19,20].

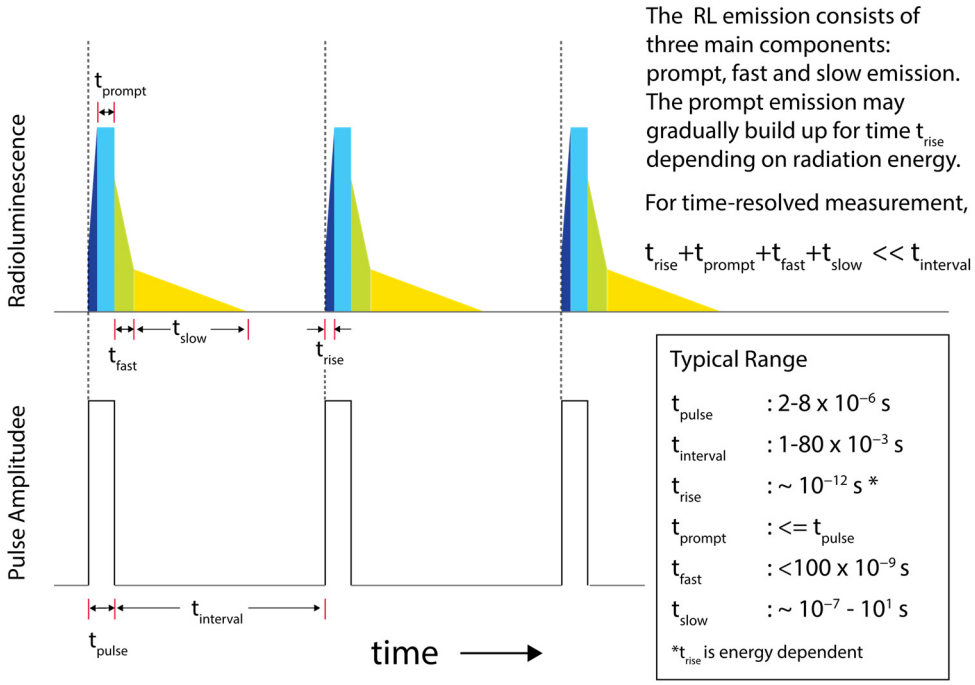

Figure 1. Diagram of time-resolved scintillation signal with general shape and timing characteristics, shown against corresponding linac pulses.

In this paper, we report on the influence of the composition of Ge dopants and fiber geometry in Ge-doped silica optical fiber scintillators used for RL based time-resolved dosimetry. The primary objective is to produce an optical fiber structure that facilitates short decay times with a sufficiently large yield for time-resolved dosimetry.

2. Materials & Methods

2.1. Scintillator Design and Fabrication

It is important to choose a scintillator with high RL yield, obtained using scintillating inorganic materials [16,21] and fast temporal RL response for time-resolved dosimetry, also allowing for good spatial resolution. The presently studied radiation-sensitive optical fiber tips used as scintillators were of submillimeter diameter and millimetre length, offering high spatial resolution measurement [1,22,23]. In this work, use has been made of various Ge-doped silica optical fiber scintillators of different core and cladding sizes. Categorized as small core (SCF) and large core fiber (LCF), the designation denotes different dopant content, tested herein for their time-resolved RL characteristics. The bulk volume of the SCF is formed of the undoped SiO_2 matrix, while the bulk of LCF is due to the Ge-doped SiO_2 network, visualized in Figure 2. In both cases, the undoped region serves as the cladding.

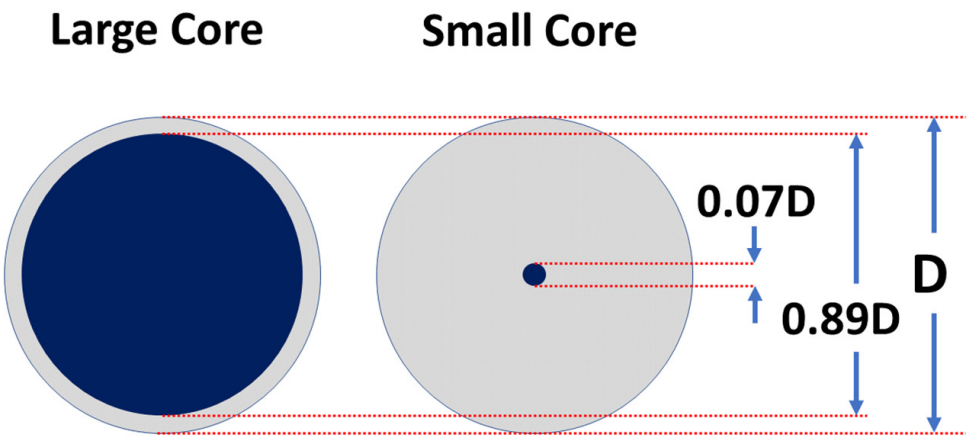

Figure 2. Visual comparison of relative core sizes of the SCF and LCF samples.

Table 1 details the properties of the optical fiber scintillator samples under test, all fabricated using the chemical vapor deposition method and pulled into the required sizes as detailed by [8,24] Each optical fiber scintillator, 20 mm in length, was hand polished at each end using a figure-of-eight motion on 30 µm and 6 µm diamond lapping film (Thorlabs®, Newton, NJ, USA).

Table 1. Dimensions of the optical fiber scintillator samples.

Core Type	Sample Codename	Outer Diameter (µm)	Inner Diameter (µm)	Core to Cladding Ratio	Germanium Concentration (wt%)
Small core	SCF 500	477	34.6	0.073	0.85
	SCF 700	713	52.6	0.074	0.91
	SCF 1000	978	64.5	0.066	0.95
Large core	LCF 500	500	449	0.898	3.05
	LCF 640	649	582	0.897	3.17
	LCF 1000	994	888	0.893	3.51

2.2. Scintillator Probe

The scintillator probe is made of insensitive radiation material, desirable in minimizing noise that can add to the RL signal from the scintillator. Polyoxymethylene (POM), an organic material has been tested at room temperature and demonstrated to be non-luminescent when exposed to ambient light and background radiation [21,25,26]. The scintillator probe is made from a 1 m long black POM rod of outer diameter 5 mm, cut into 40 mm samples, and polished at both ends. The two ends were drilled to accommodate the scintillator and polymethylmethacrylate (PMMA) core waveguiding optical fiber manufactured by Mitsubishi Chemicals, Tokyo, Japan (Super ESKA™ 4001, 920–1040 µm core, 940–1060 µm cladding, 15 m length, NA-0.5, Cladding Material-Fluorinated Polymer, Core Refractive Index-1.49, 2.2 mm outer diameter Polyethylene Jacket). The PMMA is chosen for its material flexibility and low cost over standard multimode fibers, which tend to be brittle, as well as relatively expensive. The schematic of Figure 3 shows the scintillator probe, housing the butt-coupled scintillating optical fiber and PMMA [2], allowing different samples of similar sizes to be interchanged.

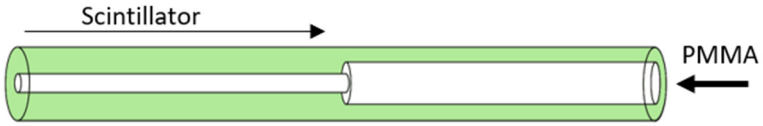

Figure 3. Schematic of the scintillator probe.

2.3. Experimental Setup

To inhibit exposure to ambient light, the optical fiber scintillator samples are housed in a sealed light-tight probe, which is then coupled to the PMMA optical fiber. To reduce the possible exposure of the bare fiber (PMMA) to the field, the sensitive optical fiber tip is placed 4 cm into a standard 10 × 10 cm^2 radiation field, at a source-to-surface distance (SSD) of 100 cm. The scintillator probe is placed in superflab^{TM} (a solid-form bolus medium manufactured by Mick Radio-Nuclear Instruments, Inc, Mount Vernon, NY, USA) that provides full-scatter conditions and build-up of the radiation dose close to the surface. The advantage of using such bolus material is that the design further optimizes dose absorption [27,28] and conforms to a variety of uneven surface geometries that eliminates air gaps.

The time-resolved RL measurement was carried out using an optical fiber-based radiation dosimetry system as shown in Figure 4. The luminescence from the optical fiber scintillators propagates along the PMMA optical fiber to the measurement system. The acquisition system comprises an analogue output photomultiplier tube (Hamamatsu H7422-40), coupled to a transimpedance amplifier and counting unit. Data acquisition gate times were varied between 1 μs and 100 μs for various analyses. The collection of data was made using a LabView-based GUI. Bremsstrahlung irradiation was produced by a linac operating at 6 MV. The linac system includes a transmission ionization chamber mounted on the treatment head to control dose delivery [29,30]. Typically, in radiotherapy practice, the linac dose rate is represented by monitor unit per minute (MU/min) which is calibrated to 1 MU = 1 cGy at the depth of maximum dose under reference conditions. The dose rate is controlled by the pulse repetition frequency (PRF) and nominal beam energy. One possible combination is a PRF of 400 Hz and a dose rate of 590 cGy/min, with a pulse width of some 3–5 μs.

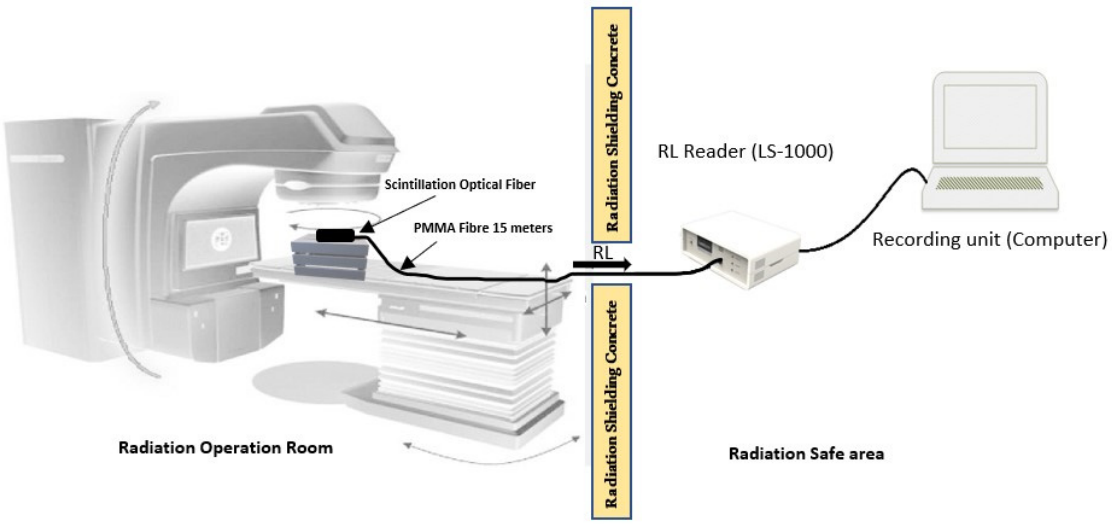

Figure 4. Experimental setup used for dosimetric characterization.

2.4. Characterization

2.4.1. RL Response and Dose-Rate Dependence

For RL response, each sample was exposed to a range of doses that in practice are typically administered in external beam fractionation, namely 35, 70, 140, 280 and 590 MU/min for a constant duration of 40 s. At such dose rates, the expected doses are of the order of 0.23, 0.46, 0.93, 1.86, and 3.93 Gy. During the exposures the RL response was measured in real-time, the intended doses being attained at a fixed exposure time of 40 s at various dose rates [31,32]. In studies of dependence on dose-rate, a fixed dose of 0.5 Gy was delivered, setting the dose value at 50 MU with dose rates of 35, 70, 140, 280, and 590 cGy/min.

2.4.2. Time-Resolved Assessment

The ability of the optical fiber scintillator samples to provide time-resolved radiation dosimetry measurements [19,33] was tested by reducing the gating time, starting initially at 100 μs, subsequently reduced to 1 μs. At such short gating times, it is possible to achieve high temporal resolution measurements at different dose rates, ranging between 590 MU/min and 35 MU/min. In using the high temporal resolution measurements, the rise time and decay time has been analyzed at the level of the individual pulse.

3. Results and Discussion

The RL response (gate time 100 μs) from the different dimension LCF and SCF samples are shown, respectively, in Figures 5 and 6. The individual graphs show RL responses for fixed duration exposures and at a fixed dose for a range of dose rates. The results displayed in Figure 5 for 6 MV photon radiation was delivered at 35, 70, 140, 280 and 590 MU/min for a constant duration of 40 s. At such dose rates, the expected doses are of the order of 0.23, 0.46, 0.93, 1.86, and 3.93 Gy. In Figure 6, a fixed dose of 0.5 Gy was delivered, setting the dose value at 50 MU. The uncertainty can be observed at <1% with an almost flat trace for a given dose rate for both LCF and SCF. However, the SCF are observed to suffer from memory effects at high dose rates. The difference is more pronounced than that observed in [34], taking close to 30 s to stabilize. This effect is not observed in sample SCF500.

Figure 7 demonstrates the normalized radioluminescence (RL) at various dose rates for both LCF and SCF samples. The dose delivery was at different dose rates of 35, 70, 140, 280 and 590 MU/min for a constant duration of 40 s, with expected doses of 0.23, 0.46, 0.93, 1.86, and 3.93 Gy, respectively. Normalization of values was carried out with reference to the RL response of the samples at the lowest dose rate of 35 MU/min. As the dose rate increases, The RL level of the LCF maintains a linear response with the index of the dependent variable at 0.96 (≈1), while the SCF is seen to suffer a loss of luminescence with an index of that at 0.87. The best fit line (following power law) and the corresponding equation has been suggested and selected by standard MS Excel function based on the data points. This behavior mandates the use of appropriate co-efficient for correction when using the SCF. An index of 0.87 represents a loss of up to 22% luminescence per pulse in the higher dose rates (example, RL response at 590 MU/min as compared to that at 35 MU/min is 13.1 times greater, instead of the expected 16.85). Due to the behavior following a power law, the loss is more pronounced as dose rates are increased. In the following few paragraphs, we will discuss in more detail the treatment of this behavior.

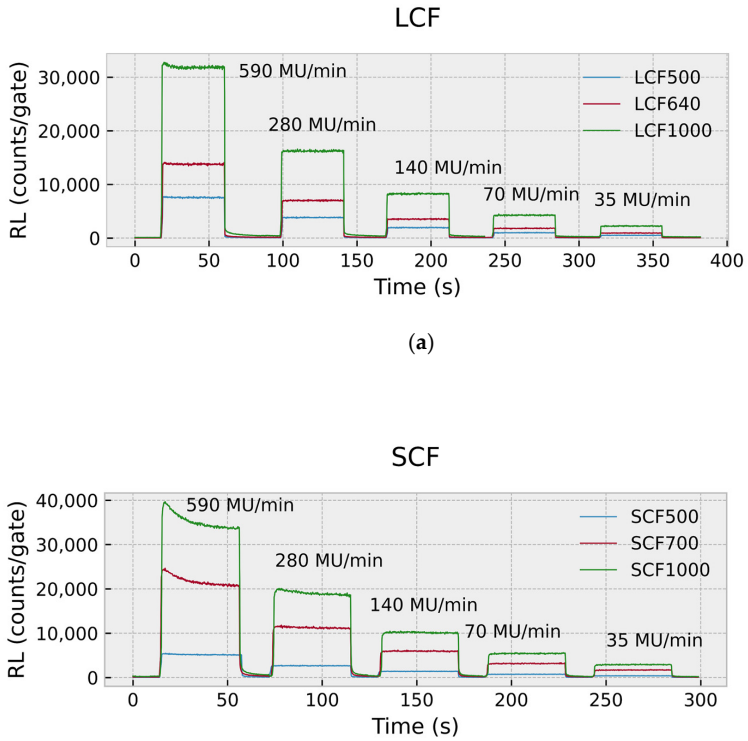

Figure 5. RL response (gate time of 100 μs) of the (**a**) LCF and (**b**) SCF samples exposed at a fixed duration of 40 s.

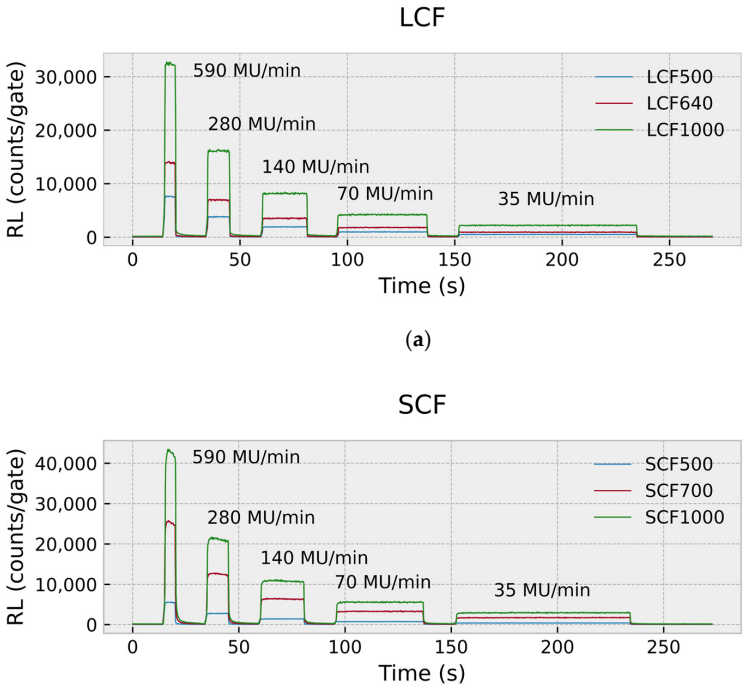

Figure 6. RL response (gate time of 100 μs) of the (**a**) LCF and (**b**) SCF samples exposed at a fixed dose of 0.5 Gy.

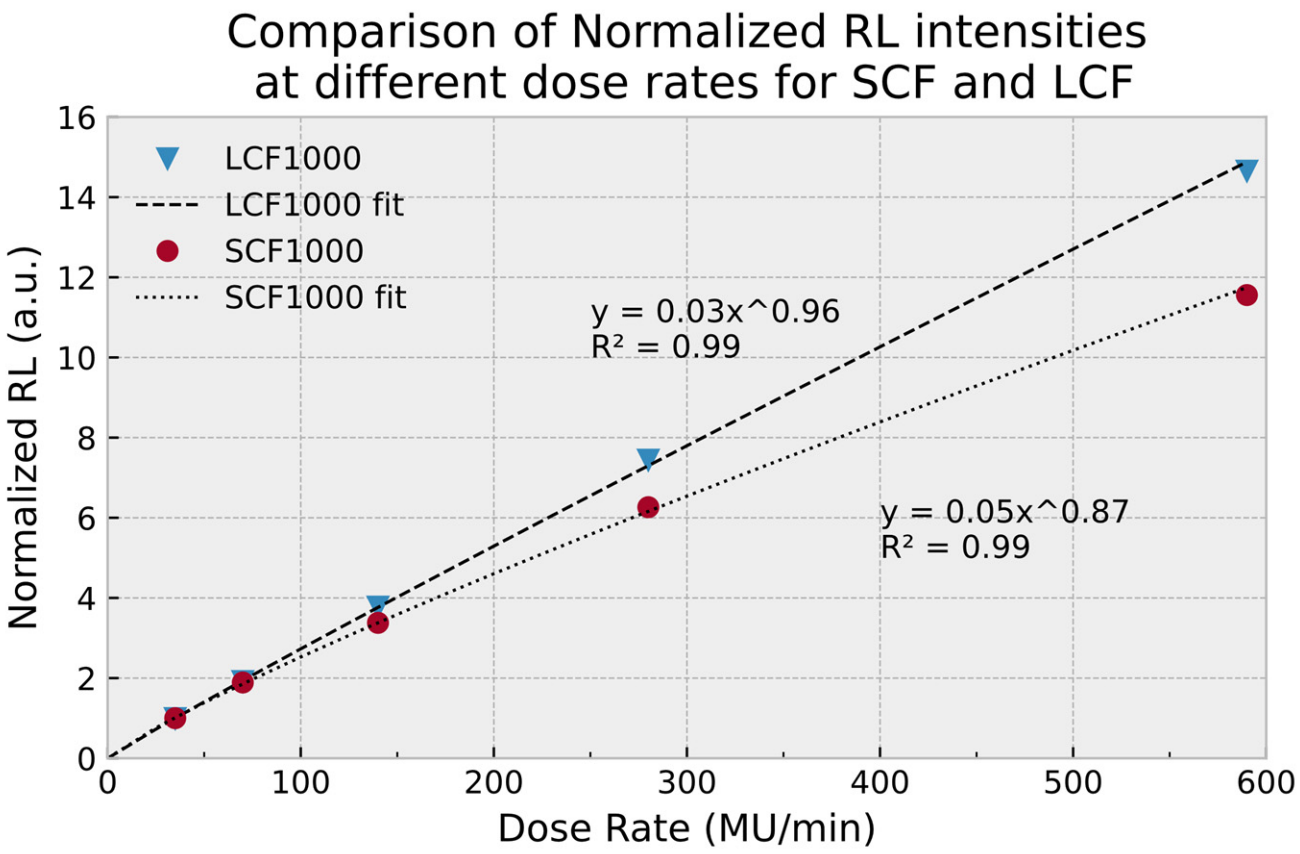

Figure 7. Normalized RL response/gate for SCF and LCF samples at various dose rates. Values are normalized to the response at lowest dose rate of 35 MU/min.

The pulse response or RL yield per gating time of 100 μs from two different sizes of LCF and SCF samples are shown in Figure 8. As has been described previously, the SCF samples yield a greater luminescence response at any given dose rate. The differences have been further analyzed using time-resolved responses capturing signals at high temporal resolution (with gate time down to 1 μs). In relative terms, for a 100 μs gating time, the total counts per pulse for SCF and LCF samples, respectively, were 530 ± 55, and 400 ± 40, both samples of overall fiber diameter of 1 mm, the results being obtained for a single pulse from a pulse train of 400 Hz. Figure 9 shows the overlapping traces of the responses from the SCF and LCF samples. From this direct comparison, the effect of Ge-doping on the RL emission is indicative of a reduction in decay time, while elevating the emission intensity. While the decay time of the LCF is given by the duration it takes for the trace to reach a value of zero, the complete decay of SCF is not directly observed and the decay time requires an estimation procedure due to its long phosphorescence. To estimate the decay time of the SCF response, a derivative of the best-fit equation of the data points of a single pulse has been taken, and the point when the change in response is less than 1 has been designated as the decay lifetime. This is also verified by analyzing the response from the final linac pulse, emulating a single X-ray pulse exposure, following the process detailed in [19].

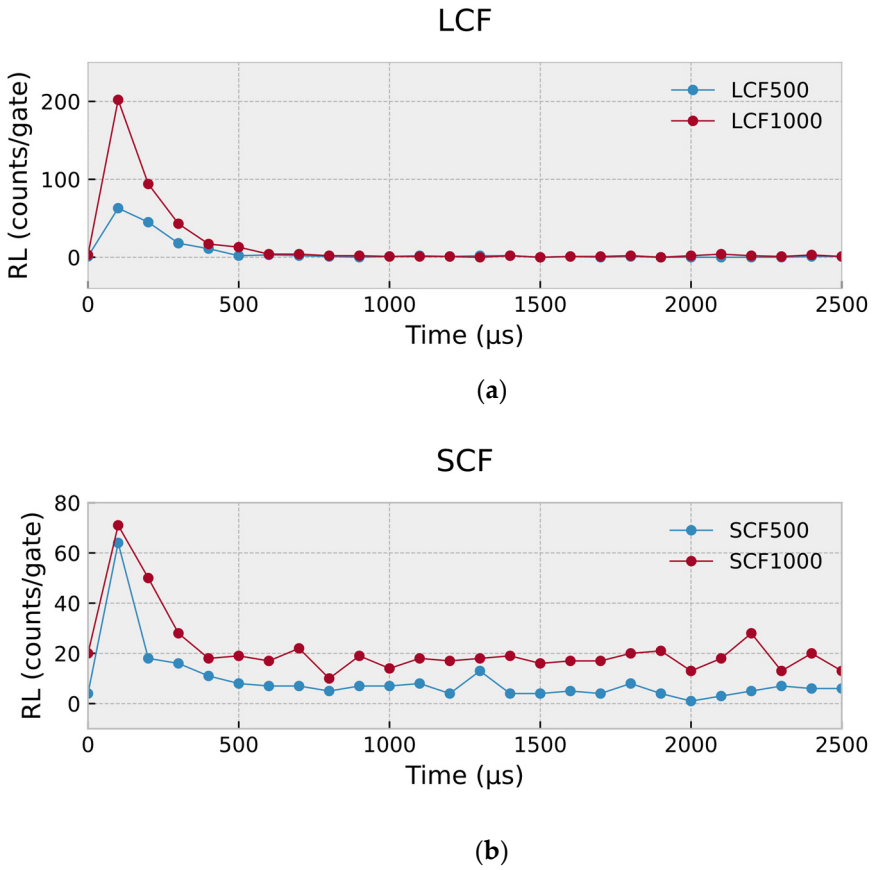

Figure 8. RL yield per gating time of 100 μs during a single pulse for (**a**) LCF samples (**b**) SCF samples at 590 MU/min.

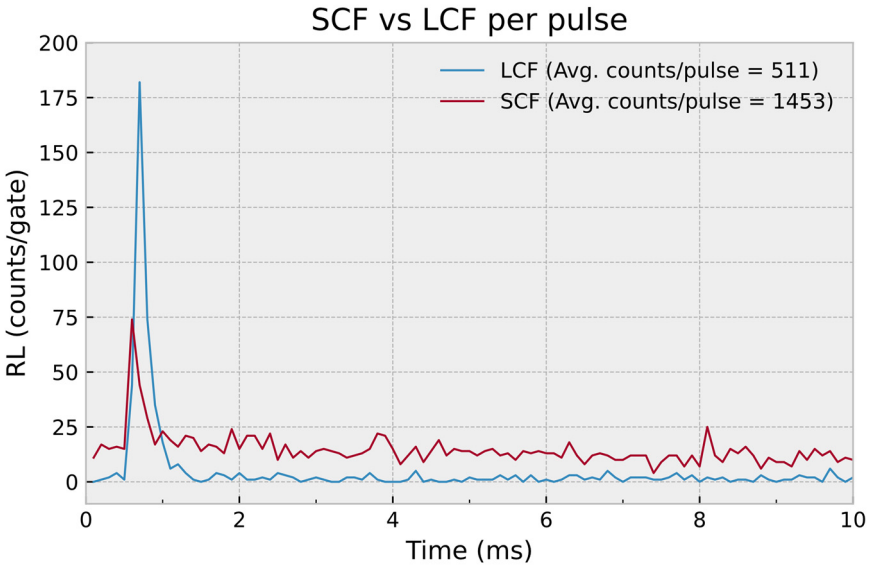

Figure 9. Comparison of the traces of the RL response (gate time of 100 μs) from a single pulse for the SCF and LCF obtained at dose rates of 140 MU/min (10 ms interval between adjacent pulses).

Figure 10 shows the progression of the accumulated counts for SCF and LCF, constructed from data collected with a gate time of 1 μs. The reference trace, from the PMMA fiber, corresponds to the stem effect as acquired from a bare PMMA without an attached

scintillator. The data has been normalized to the stable reading from the PMMA which is reached after 4 μs. The steep rise over the first 4 μs corresponds to the linac pulse ON time, where all three fibers produce comparable yield, pointing towards the dominating effect of the stem signal. The emission from the stem effect subsides almost instantaneously when the linac pulse switches OFF. Beyond that point, the recorded counts are a result of the RL signal from the scintillating fibers. The LCF climbs to a slightly greater accumulated reading as compared to the SCF during the first 100 μs, as can be observed from Figure 10. While the LCF approaches a stable reading at some 600 μs, the SCF emission prevails until 2.5 ms—the point at which the next pulse is expected for PRF of 400 Hz. The SCF continues to yield greater luminescence beyond 800 μs, predominantly contributed to by the phosphorescent component of the RL signal. At lower dose rates, the SCF may accumulate two or three times more luminescence per pulse due to this phosphorescent emission. The time axis of Figure 10 is presented in log scale to visualize the luminescence trend in the first few μs and the last few hundred μs. Normalization of the values to that of the PMMA at a stable point (corresponding also to the duration of the pulse, ≈4 μs) enables estimating the proportion of luminescent signal produced solely by the scintillating material. From the given figure, the LCF reaches about 115% and the SCF reaches about 155% of the stem signal level. The additional 15% and 55% of luminescence from the LCF and SCF, respectively, would contribute to information relevant to dosimetry. As will be discussed next, the comparatively lower yield from the LCF is practically more viable owing to the timing characteristics of the signal. Bradley et al. [35] have discussed one possible effect of dose rate dependence of the output from optical fibers of similar structure to the SCF, the total accumulated counts being observed to be 10–15% greater at lower rates than that at higher dose rates, rendering the need for correction factors.

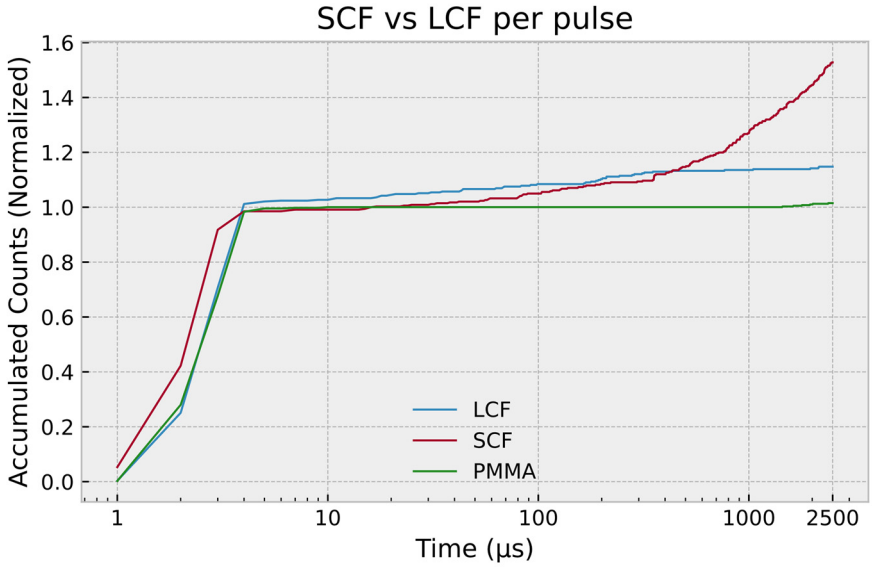

Figure 10. Normalized accumulated counts (gate time of 1 μs) with respect to time. Values are normalized to the total response of the PMMA carrier fiber during radiation exposure (≈4 μs).

Moreover, the earlier discussion highlighted the signal build-up phenomenon, with materials having long phosphorescence characteristics [36]. As shown in Figure 11, the counts recorded per pulse is adversely affected by the phosphorescent signal from preceding pulses, particularly at high dose rates, making the material limited to use for low dose rate applications only. Results from the present study show this phenomenon to be present predominantly in the SCF samples, suggesting a role of the dominant SiO_2 matrix present in the cladding of such a sample. The recorded total counts per pulse show a 30% drop for SCF when irradiated at a higher dose rate, while the LCF maintains a consistent reading at both dose rates (35- and 590 MU/min).

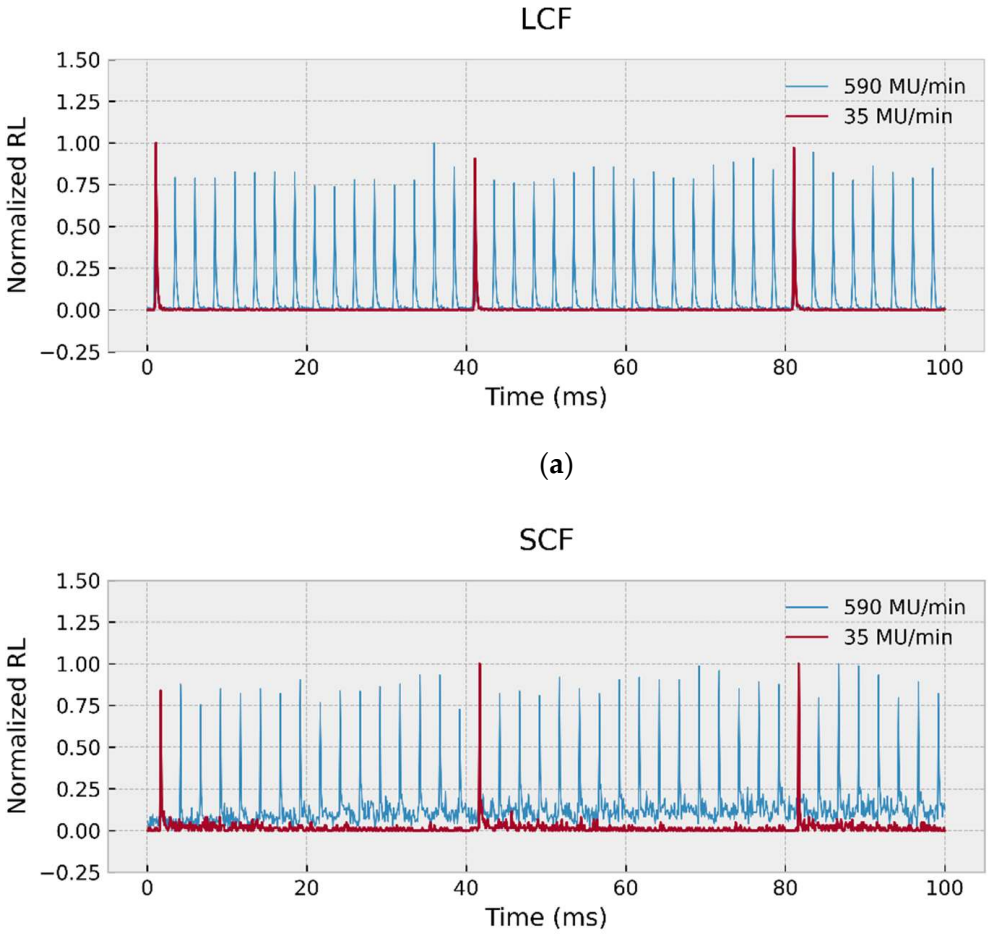

Figure 11. Pulse train of the RL response (gate time of 100 µs) at 35 MU/min and 590 MU/min for (**a**) LCF and (**b**) SCF, highlighting the long phosphorescence presence in SCF. Values are normalized to the highest y-axis value for the datastream.

The results also suggest a contribution of Ge-doping in affecting the triplet states of the SiO_2 matrix, thereby reducing phosphorescence effects. This is a desirable feature of scintillating glass materials as has been discussed by [19]. The estimated decay time of the SCF is 59 ms, and that of LCF is 0.6 ms from Figures 9 and 11. The SCF, with its structure similar to P-doped [34] and Ge-doped [12] cylindrical fiber, has a decay time in the range of tens of ms. Doping a larger volume of the silica matrix, i.e., extending the size of the doped core in relation to the fiber's overall diameter, shortens the decay time substantially, enabling time-resolved measurements in medical dosimetry.

4. Conclusions

We report on the influence of Ge dopants in Ge-doped silica optical fiber scintillators used for radioluminescence (RL) based time-resolved dosimetry, in particular the decay time and RL yield. The Ge-doped silica optical fiber scintillator with large and small core samples represents high and low Ge-dopant contents. The samples showed linear RL response, with differing memory and afterglow effects. The large core samples, indicative of a higher Ge-doping content and a high number of defects, demonstrate faster decay time and higher RL yield. The results suggest a contribution of Ge-doping in affecting the triplet states of the SiO_2 matrix, thereby reducing phosphorescence effects. This is a desirable feature of scintillating glass materials that help avoid the pulse pile-up effect,

especially in high dose-rate applications. The primary objective to produce a structure that facilitates short decay times with a sufficiently large yield for time-resolved dosimetry has been achieved in this study with Ge-doped optical fiber scintillators with a large core-to-cladding ratio.

Author Contributions: Z.H.T., A.O., A.A., A.B., H.M.Z., H.A.A.-R. and D.A.B. designed and carried out the experiments at the linac facility. H.M.Z. and A.A. have also provided practical consultation regarding the functionality of the linac. K.Y.C. contributed to the instrumentation of the system and the discussion of results. S.A.I. contributed to the optical characterization and analysis of the samples. Data processing, visualization, and analysis were conducted by Z.H.T., A.O. and A.B. The original manuscript has been drafted by Z.H.T., A.O., A.B. and H.A.A.-R. The original manuscript has been thoroughly revised by H.A.A.-R. and D.A.B. All authors have read and agreed to the published version of the manuscript.

Funding: We are grateful for grant support from MOSTI, Malaysia ICF (MMUE/190082).

Acknowledgments: The authors would like to thank Sayuti Jamaudin, Nurul Aini Mohd Noor, Izzatie Razak and Syafiq Johari from the Multimedia University for their tremendous support on project management, and arrangement of research trips.

Conflicts of Interest: The authors have no conflict of interest to declare.

References

1. Goulet, M.; Archambault, L.; Beaulieu, L.; Gingras, L. 3D Tomodosimetry Using Long Scintillating Fibers: A Feasibility Study. *Med. Phys.* **2013**, *40*, 101703. [CrossRef] [PubMed]
2. Elsey, J.; McKenzie, D.R.; Lambert, J.; Suchowerska, N.; Law, S.L.; Fleming, S.C. Optimal Coupling of Light from a Cylindrical Scintillator into an Optical Fiber. *Appl. Opt.* **2007**, *46*, 397–404. [CrossRef] [PubMed]
3. Williams, M.V. Radiotherapy Near Misses, Incidents and Errors: Radiotherapy Incident at Glasgow. *Clin. Oncol.* **2007**, *19*, 1–3. [CrossRef] [PubMed]
4. Di Martino, F.; Barca, P.; Barone, S.; Bortoli, E.; Borgheresi, R.; De Stefano, S.; Di Francesco, M.; Faillace, L.; Giuliano, L.; Grasso, L.; et al. FLASH Radiotherapy With Electrons: Issues Related to the Production, Monitoring, and Dosimetric Characterization of the Beam. *Front. Phys.* **2020**, *8*, 481. [CrossRef]
5. Beddar, A.S.; Kinsella, K.J.; Ikhlef, A.; Sibata, C.H. A Miniature "Scintillator-Fiberoptic-PMT" Detector System for the Dosimetry of Small Fields in Stereotactic Radiosurgery. *IEEE Trans. Nucl. Sci.* **2001**, *48*, 924–928. [CrossRef]
6. Cho, J.D.; Son, J.; Sung, J.; Choi, C.H.; Kim, J.S.; Wu, H.; Park, J.M.; Kim, J. Flexible Film Dosimeter for in Vivo Dosimetry. *Med. Phys.* **2020**, *47*, 3204–3213. [CrossRef]
7. Boadu, M.; Rehani, M.M. Unintended Exposure in Radiotherapy: Identification of Prominent Causes. *Radiother. Oncol.* **2009**, *93*, 609–617. [CrossRef]
8. Mahdiraji, G.A.; Adikan, F.R.M.; Bradley, D.A. Collapsed Optical Fiber: A Novel Method for Improving Thermoluminescence Response of Optical Fiber. *J. Lumin.* **2015**, *161*, 442–447. [CrossRef]
9. Correia, A.; Pirraco, R.; Rosa, C.C.; Chiquita, S.; Hussain, N.S. A Multi-Sensor Dosimeter for Brachytherapy Based on Radioluminescent Fiber Sensors. *Fifth Eur. Workshop Opt. Fibre Sens.* **2013**, *8794*, 87941S. [CrossRef]
10. Lambert, J.; McKenzie, D.R.; Law, S.; Elsey, J.; Suchowerska, N. A Plastic Scintillation Dosimeter for High Dose Rate Brachytherapy. *Phys. Med. Biol.* **2006**, *51*, 5505–5516. [CrossRef]
11. Therriault-Proulx, F.; Briere, T.M.; Mourtada, F.; Aubin, S.; Beddar, S.; Beaulieu, L. A Phantom Study of an in Vivo Dosimetry System Using Plastic Scintillation Detectors for Real-Time Verification of 192Ir HDR Brachytherapy. *Med. Phys.* **2011**, *38*, 2542–2551. [CrossRef] [PubMed]
12. Rahman, A.K.M.M.; Begum, M.; Begum, M.; Zubair, H.T.; Abdul-Rashid, H.A.; Yusoff, Z.; Bradley, D.A. Radioluminescence of Ge-Doped Silica Optical Fibre and Al_2O_3:C Dosimeters. *Sens. Actuators A Phys.* **2018**, *270*, 72–78. [CrossRef]
13. Archer, J.; Li, E.; Petasecca, M.; Dipuglia, A.; Cameron, M.; Stevenson, A.; Hall, C.; Hausermann, D.; Rosenfeld, A.; Lerch, M. X-Ray Microbeam Measurements with a High Resolution Scintillator Fibre-Optic Dosimeter. *Sci. Rep.* **2017**, *7*, 1–7. [CrossRef]
14. Laissue, J.A.; Lyubimova, N.; Wagner, H.-P.; Archer, D.W.; Slatkin, D.N.; Di Michiel, M.; Nemoz, C.; Renier, M.; Brauer, E.; Spanne, P.O.; et al. Microbeam Radiation Therapy. In *Medical Applications of Penetrating Radiation*; Barber, H.B., Roehrig, H., Eds.; International Society for Optics and Photonics: Bellingham, WA, USA, 1999; p. 38.
15. Velthuis, J.J.; Page, R.F.; Purves, T.M.; Beck, L.; Hanifa, M.A.M.; Hugtenburg, R.P. Toward Pulse by Pulse Dosimetry Using an SC CVD Diamond Detector. *IEEE Trans. Radiat. Plasma Med. Sci.* **2017**, *1*, 527–533. [CrossRef]
16. Van Eijk, C.W.E. Inorganic Scintillators in Medical Imaging. *Phys. Med. Biol.* **2002**, *47*, R85–R106. [CrossRef]
17. Basaif, A.; Oresegun, A.; Tarif, Z.H.; Zin, H.; Choo, K.Y.; Ibrahim, S.A.; Abdul-Rashid, H.A.; Bradley, D.A. Ge-Doped Silica Optical Fibre for Time Resolved Radiation Dosimetry. *Radiat. Phys. Chem.* **2021**, *189*, 109669. [CrossRef]

18. Mizanur Rahman, A.K.M.; Zubair, H.T.; Begum, M.; Abdul-Rashid, H.A.; Yusoff, Z.; Ung, N.M.; Mat-Sharif, K.A.; Wan Abdullah, W.S.; Amouzad Mahdiraji, G.; Amin, Y.; et al. Germanium-Doped Optical Fiber for Real-Time Radiation Dosimetry. *Radiat. Phys. Chem.* **2015**, *116*, 170–175. [CrossRef]
19. Justus, B.L.; Falkenstein, P.; Huston, A.L.; Plazas, M.C.; Ning, H.; Miller, R.W. Gated Fiber-Optic-Coupled Detector for In Vivo Real-Time Radiation Dosimetry. *Appl. Opt.* **2004**, *43*, 1663. [CrossRef]
20. Teichmann, T.; Sponner, J.; Radtke, J.; Henniger, J. Gated Discrimination of the Stem Signal in Pulsed Radiation Fields for a Fiber Optic Dosimetry System Based on the Radioluminescence of Beryllium Oxide. *Radiat. Meas.* **2017**, *106*, 552–555. [CrossRef]
21. Lecoq, P.; Annenkov, A.; Gektin, A.; Korzhik, M.; Pedrini, C. Inorganic Scintillators for Detector Systems. In *Particle Acceleration and Detection*; Springer: Berlin/Heidelberg, Germany, 2006; pp. 81–122. ISBN 3-540-27766-8.
22. Lam, S.E.; Bradley, D.A.; Mahmud, R.; Pawanchek, M.; Abdul Rashid, H.A.; Mohd Noor, N. Dosimetric Characteristics of Fabricated Ge-Doped Silica Optical Fibre for Small-Field Dosimetry. *Results Phys.* **2019**, *12*, 816–826. [CrossRef]
23. Butson, M.J.; Rozenfeld, A.; Mathur, J.N.; Carolan, M.; Wong, T.P.Y.; Metcalfe, P.E. A New Radiotherapy Surface Dose Detector: The MOSFET. *Med. Phys.* **1996**, *23*, 655–658. [CrossRef] [PubMed]
24. Entezam, A.; Khandaker, M.U.; Amin, Y.M.; Ung, N.M.; Bradley, D.A.; Maah, J.; Safari, M.J.; Moradi, F. Thermoluminescence Response of Ge-Doped Cylindrical-, Flat- And Photonic Crystal Silica-Fibres to Electron and Photon Radiation. *PLoS ONE* **2016**, *11*, 1–15. [CrossRef] [PubMed]
25. Pain, F.; Laniece, P.; Mastrippolito, R.; Charon, Y.; Comar, D.; Leviel, V.; Pujol, J.F.; Valentin, L. SIC, an Intracerebral Radiosensitive Probe for In Vivo Neuropharmacology Investigations in Small Laboratory Animals: Theoretical Considerations and Practical Characteristics. *IEEE Trans. Nucl. Sci.* **2000**, *47*, 25–32. [CrossRef]
26. Mones, E.; Veronese, I.; Vedda, A.; Loi, G.; Fasoli, M.; Moretti, F.; Chiodini, N.; Cannillo, B.; Brambilla, M. Ce-Doped Optical Fibre as Radioluminescent Dosimeter in Radiotherapy. *Radiat. Meas.* **2008**, *43*, 888–892. [CrossRef]
27. Hugtenburg, R.P.; Johnston, K.; Chalmers, G.J.; Beddoe, A.H. Application of Diamond Detectors to the Dosimetry of 45 and 100 KVp Therapy Beams: Comparison with a Parallel-Plate Ionization Chamber and Monte Carlo. *Phys. Med. Biol.* **2001**, *46*, 2489–2501. [CrossRef] [PubMed]
28. Smith, K.; Balter, P.; Duhon, J.; White, G.A.; Vassy, D.L.; Miller, R.A.; Serago, C.F.; Fairobent, L.A. AAPM Medical Physics Practice Guideline 8.a.: Linear Accelerator Performance Tests. *J. Appl. Clin. Med. Phys.* **2017**, *18*, 23–39. [CrossRef]
29. Leybovich, L.B.; Sethi, A.; Dogan, N. Comparison of Ionization Chambers of Various Volumes for IMRT Absolute Dose Verification. *Med. Phys.* **2003**, *30*, 119–123. [CrossRef]
30. Low, D.A.; Parikh, P.; Dempsey, J.F.; Wahab, S.; Huq, S. Ionization Chamber Volume Averaging Effects in Dynamic Intensity Modulated Radiation Therapy Beams. *Med. Phys.* **2003**, *30*, 1706–1711. [CrossRef]
31. Bradley, D.A.; Khandaker, M.U.; Alanazi, A. Irradiated Glass and Thermoluminescence Yield: Dosimetric Utility Reviewed. *Radiat. Phys. Chem.* **2020**, *170*, 108680. [CrossRef]
32. Almond, P.R.; Biggs, P.J.; Coursey, B.M.; Hanson, W.F.; Huq, M.S.; Nath, R.; Rogers, D.W.O. AAPM's TG-51 Protocol for Clinical Reference Dosimetry of High-Energy Photon and Electron Beams. *Med. Phys.* **1999**, *26*, 1847–1870. [CrossRef]
33. Tanyi, J.A.; Krafft, S.P.; Ushino, T.; Huston, A.L.; Justus, B.L. Performance Characteristics of a Gated Fiber-Optic-Coupled Dosimeter in High-Energy Pulsed Photon Radiation Dosimetry. *Appl. Radiat. Isot.* **2010**, *68*, 364–369. [CrossRef] [PubMed]
34. Zubair, H.T.; Oresegun, A.; Rahman, A.K.M.M.; Ung, N.M.; Mat Sharif, K.A.; Zulkifli, M.I.; Yassin, S.Z.M.; Maah, M.J.; Yusoff, Z.; Abdul-Rashid, H.A.; et al. Real-Time Radiation Dosimetry Using P-Doped Silica Optical Fiber. *Measurement* **2019**, *146*, 119–124. [CrossRef]
35. Bradley, D.A.; Zubair, H.T.; Oresegun, A.; Louay, G.T.; Abdul-Rashid, H.A.; Ung, N.M.; Alzimami, K.S. Towards the Development of Doped Silica Radioluminescence Dosimetry. *Radiat. Phys. Chem.* **2019**, *154*, 46–52. [CrossRef]
36. Bradley, D.A.; Zubair, H.T.; Oresegun, A.; Louay, G.T.; Zin, H.M.; Ung, N.M.; Abdul-Rashid, H.A. Time-Resolved Dose Measurements of Linear Accelerator Pulses Using a Fibre Optic Sensor: Applications and Challenges. *Radiat. Phys. Chem.* **2020**, *167*, 108212. [CrossRef]